An IMU-based System Identification Technique for Quadrotors

Vahid Khorani, Naeem Ajilforoushan
Mechatronics Research Laboratory (MRL)
Qazvin Islamic Azad University (QIAU)
Qazvin, Iran
vahid.khorani@gmail.com , n.ajilforoushan@gmail.com

Alireza Mohammad Shahri
Electrical Engineering Department
Iran University of Science and Technology (IUST)
Tehran, Iran
shahri@iust.ac.ir

***Abstract*—Accurate system identification has an important role in designing high-performance controllers for robotic platforms. Most advanced controllers are designed based on the plants' dynamic models and their identified parameters. However, some models and their parameters change because of payload or condition variations. Online identification of these changes leads to develop high performance adaptive controllers. In this research, a rigorous amount of study is carried out to identify the parametric variations of a multi-rotor using a sensory system. The proposed method applies an inertial measurement unit (IMU) to identify the exact center of mass and its displacements. This method, which is based on the genetic algorithm (GA), is independent of the IMU location. The proposed algorithm is theoretically investigated while experimental results are presented to validate the performance of the algorithm.**

Quadrotor, Parameter Identification, IMU, GA

I. INTRODUCTION

Quadrotors are an emerging rotorcraft concept for unmanned aerial vehicle (UAV) platforms. The vehicle consists of four motors in total, with two pairs of counter-rotating and fixed-pitch blades located at the four corners of the aircraft [1]. Having four motors, the quadrotor can be controlled and stabilized without swash plates. Accordingly, unlike helicopters it is not necessary to change the pitch angle of the blades in the quadrotor's control system.

Despite their simple mechanical design, the quadrotors have nonlinear and complicated dynamic behavior. Moreover, these vehicles, with four actuators and six degrees of freedom, are classified as under-actuated platforms. Therefore, it is a relatively difficult task to design a controller for these systems [2]. Therefore, many types of control techniques are proposed for these plants. The proposed algorithms might be categorized in non-model and model based controllers. As an non-model based controller, T. Bresciani et al. [3] propose a PID controller for their quadrotor platform. In their research, four separate controllers are integrated to control the vehicle's attitude and altitude movements. S. Bouabdallah at al. [4] test both PD and PID controllers. These controllers are tuned using a simulated quadrotor and applied on an OS4 platform. PD^2 and nonlinear PI/PID [5, 6] controllers are also applied on quadrotors. Mostly, these controllers are tuned on real platforms [7]. Similarly, S. Bouabdallah et al. [4] test a model based LQ controller. Results show, using an LQ controller, it will be unavoidable to model the whole quadrotor's subsystems. Nonlinear, backstepping, sliding mode, and LPV controllers are also applied on Quadrotors [8, 9]. Results show that the most model based controllers are severely dependent on the precision of the model and its parameters.

Modeling the quadrotor's dynamic behavior and identifying its parameters are inevitable for model based controllers [10]. Accordingly, some researchers have studied the quadrotor's dynamic model and introduced their models based on both Newton-Euler and Lagrangian methods [3, 8, 11]. P. Martin et al. [12] propose a more detailed model. However, the parameters of the quadrotor's dynamic model may change depending on different missions and configurations. In addition, the accuracy of the modeling procedure is affected by uncertainties. Therefore, the model based controllers should be updated in real time in order to have a better performance. As a solution, some researchers have applied more intelligent, adaptive, and robust controllers including: direct adaptive sliding mode controllers, robust controllers, fuzzy and neural network based controllers [2, 13, 14]. Although these advanced controllers present better performance, as another solution, real-time estimating and updating of the parameters leads to a simpler controller while having good performance. As an example, researchers of [15] state that finding the exact center of mass is considerably helpful for designing a better and simpler controller for quadrotors. Moreover, in some applications the parameter variations are significant as the robot is used to carry weighty and complicated burdens.

In this research a real-time GA-based method is proposed to identify the quadrotor's parameters. It is shown that the values measured by inertial sensors installed on a quadrotor platform can be used to identify and update the location of the center of mass.

II. THEORETICAL BACKGROUND

The quadrotor's dynamic model and the Strapdown inertial navigation equations are the fundamental concepts which are used in this research.

A. *Quadrotor's Dynamic Model*

Neglecting the quadrotor's drag force, it is possible to model the dynamic behavior of the platform as a 6-DOF rigid

978-1-4673-6315-0/13/$31.00 ©2013 IEEE

body [3, 8, 11]. Two frames named *body frame* and *world frame* are used in this modeling. Fig. 1 shows these frames and forces acting on the quadrotor. As shown in this figure, three axes x_B, y_B, and z_B form the body frame, B, which is rigidly connected to the center of mass. It is preferred that the x_B-axis indicates to the robot's forward/heading direction and the z_B-axis is perpendicular to the quadrotor plane and pointing up when the robot is hovering. The world frame, W, is defined by axes x_W, y_W, and z_W, with z_W pointing upward. Motors 1, 2, 3, and 4 are on the positive x_B-axis, positive y_B-axis, negative x_B-axis, and negative y_B-axis, respectively [11].

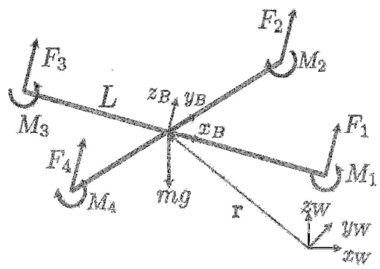

Fig. 1. Coordinate systems and forces used in modeling procedure

The equations governing the acceleration of the center of mass are

$$m\ddot{\mathbf{r}}^W = \begin{bmatrix} 0 \\ 0 \\ -mg \end{bmatrix} + \mathbf{R}_B^W \begin{bmatrix} 0 \\ 0 \\ \sum F_i \end{bmatrix} \tag{1}$$

where $\mathbf{r}^W$ is the position vector showing the center of mass and m is the mass of the vehicle.

B. *Strapdown Inertial Navigation Equations*

The linear parts of the Strapdown inertial navigation equations are presented in this section. Working in a laboratory which is limited to a small environment, we can neglect the effects of the earth rotation and its curvature from the inertial navigation equations. Accordingly, the navigation equations may be written by equation (2) which is presented by [16].

$$\ddot{\mathbf{r}}^W = \begin{bmatrix} 0 & 0 & -g \end{bmatrix}^T + \mathbf{R}_B^W \mathbf{f}^B \tag{2}$$

where $\ddot{\mathbf{r}}^W$ shows the vector of linear accelerations of the robot with respect to the world frame, g presents the acceleration due to the earth gravity, and $\mathbf{f}^B$ is the vector of accelerations measured by the accelerometers:

$$\mathbf{f}^B = \begin{bmatrix} f_x & f_y & f_z \end{bmatrix}^T \tag{3}$$

In this paper, it is more convenient to refer to the accelerometers measuring f_{x_b} and f_{y_b} as horizontal accelerometers, and to the accelerometer measuring f_{z_b} as vertical accelerometer.

III. Proposed Method

It is possible to show that the values measured by an accelerometer will be close to zero if the sensor is installed at a place close to a quadrotor's center of mass and the drag force is neglected. This fact is proven in subsection A as it is also studied in more details in a recent paper of the authors [17]. However, considering the drag force and the IMU misalignments, a real accelerometer measures some non-zero values. These values are investigated in subsection B. It is shown that these values are mainly from three sources named '*pseudo accelerations*'. We propose a formula to calculate the pseudo accelerations using a gyroscope. Some parameters including the distance between the IMU and the vehicle's mass center are used in this formula. We claim the values calculated by our formula will be equal to the values measured by a horizontal accelerometer if we can identify the parameters which are used in our formula. Therefore, a genetic algorithm is used in subsection C to fit the signal calculated by our formula and the signal measured by the horizontal accelerometer as the parameters are optimized and identified. Identifying the mentioned parameters, we can estimate the mass center displacements. Finally, another formula is proposed in subsection D to calculate the mass center displacement.

A. *Values Measured by an Accelerometer Installed Close to the Center of Mass While the Drag Force is Neglected*

The quadrotor's dynamic model and the Strapdown inertial navigation equations presented in section II are used in this section. It is worth noting that the drag force was neglected in modeling procedure. This negligence is our technique to show what happens without drag force. However, we will consider this force in next sections. It was also assumed that the accelerometers are installed at the robot's mass center. Therefore, it is possible to study the values measured by the accelerometer while the drag force is neglected and the sensors are installed in a place close to the vehicle's mass center. So, equation (1) from the quadrotor's dynamic model and equation (2) from the Strapdown equations are applied to derive following equation:

$$\begin{bmatrix} 0 \\ 0 \\ -g \end{bmatrix} + \frac{1}{m}\mathbf{R}_B^W \begin{bmatrix} 0 \\ 0 \\ \sum F_i \end{bmatrix} = \begin{bmatrix} 0 \\ 0 \\ -g \end{bmatrix} + \mathbf{R}_B^W \mathbf{f}^B \tag{4}$$

Solving this equation in order to obtain $\mathbf{f}^B$ results in:

$$\mathbf{f}^B = \begin{bmatrix} 0 & 0 & \sum \frac{F_i}{m} \end{bmatrix}^T \tag{5}$$

This result shows that the values measured by the horizontal accelerometers are zero while the quadrotor is flying. Indeed, the earth gravity and the quadrotor's linear accelerations are two acceleration sources in system above which are against each other. Therefore, the value of the overall acceleration seen by the sensors is zero.

B. *Values Measured by a Real Accelerometer Installed on a Quadrotor*

In previous section, it was shown that the values measured by a quadrotor's horizontal accelerometer will be zero if the sensor is installed at the center of mass and the drag force is neglected. However, real accelerometers measure some non-zero values as they are installed imprecisely and affected by drag forces. Therefore, it is important to find out "what are the values measured by the real accelerometer?" In order to answer this question, we studied all constitutive elements of the values measured by real accelerometers installed on the quadrotors. Based on our study, a real horizontal accelerometer is affected by five elements listed as follows:

1) the earth gravity,
2) the quadrotor's linear accelerations with respect to the body frame,
3) the effects of the quadrotor's angular accelerations when the sensor is installed far from the center of mass in an imprecise manner,
4) the effects of centrifugal forces when the sensor is installed far from the center of mass in an imprecise manner,
5) and the effects of the drag forces.

The first two elements are against each other and the overall measurement resulted by them is zero as it was studied in the previous subsection. So, our study is focused on the other elements. We name these elements '*pseudo accelerations*', because they are produced by non-inertial sources.

In this section a method is proposed in which a y_b-axis gyroscope is used to calculate the pseudo accelerations affecting on the x_b-axis accelerometer. This method is based on a formula which consists of the angular rate measured by the y_b-axis gyroscope, three parameters named *'IMU misalignments'* and a parameter named *'drag coefficient'*. *'IMU misalignments'* are the location and orientation of the IMU with respect to the center of mass and body frame and *'drag coefficient'* is the coefficient of the drag forces affecting on the quadrotor.

Prior to developing the proposed formula, let us consider some assumptions.

- It is assumed that the quadrotor's altitude is stationary.
- An intentional misalignment is applied in IMU installation and the sensor is located in a place far from the center of mass. Without this intentional misalignment the amplitude of the measured accelerations will be small and it will be difficult to remove the noise and vibration effects as we use low-quality MEMS accelerometers.
- The IMU misalignments and its distance from the center of mass are studied in x_B-z_B plane.
- It is assumed that the quadrotor flies in an indoor environment and as a result of that there is no wind affecting on the vehicle.

*We are going to break all assumptions above in our next studies.

The described system is shown in Fig. 2. The pseudo accelerations are presented in green color. According to this figure, there is an intentional misalignment in the IMU installation and it is also located in a place far from the center of mass. The center of the IMU has a distance r from the center of the body frame and there is an angle of β between the r and the x_b-axis. The IMU also has an angle of α with respect to the x_b-axis. In a precise and correct installation in which the IMU is installed at the center of mass, the physical parameters r, β, and α will be 0, $\frac{\pi}{2}$, and 0, respectively. θ in this figure shows the pitch angle around y_b-axis, ω_y shows the angular rate measured by y_b-axis gyroscope and $\bar{f}_{x_b}$ shows the pseudo accelerations measured by the accelerometer installed in x_b direction.

$\sum \frac{F_i}{m}$ is the acceleration produced by the propellers, $r\dot{\omega}_y$ is the angular acceleration due to the quadrotor's rotation around its y_b-axis and $r\omega_y^2$ is the centrifugal force applied on the IMU.

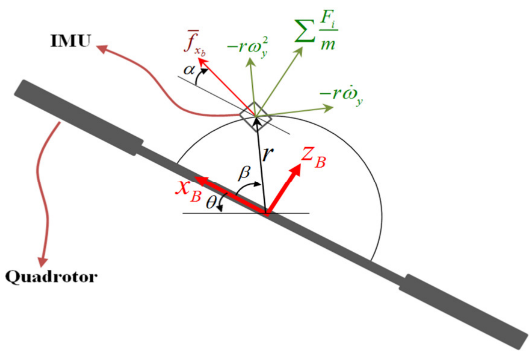

Fig. 2. The pseudo accelerations affecting on x_b-axis accelerometer

Given the assumption that the height of the quadrotor is fixed during the test and $\sum \frac{F_i}{m}$ may approximate to g, $\bar{f}_{x_b}$ in Fig. 2 can be calculated from equation below:

$$\bar{f}_{x_b} = g\sin\alpha - r\omega_y^2\cos(\beta-\alpha) + r\dot{\omega}_y\sin(\beta-\alpha) \quad (6)$$

θ can be integrated using y_b-axis gyroscope and therefore it is possible to extract equation below from the first row of equation (1):

$$v_X = g\int_0^t \sin\left(\int_0^\tau \omega_{y(\sigma)}d\sigma + \theta_0\right)d\tau + v_{X_0} \quad (7)$$

where v_X is the robot's horizontal linear velocity in x_W direction and initial values θ_0 and v_{X0} can be considered to be zero depending on the test situation.

Air resistance against the quadrotor's horizontal motion is proportional to the square of the horizontal velocity of the platform [18] and can be estimated using the following equation:

$$R_{air} = \mu v_X^2 \quad (8)$$

where μ is the drag coefficient. Finally, considering the drag force, the pseudo accelerations applied on the x_b-axis accelerometer can be calculated using equation below.

$$\bar{f}_{x_b} = g\sin\alpha - r\omega_y^2\cos(\beta-\alpha) + r\dot{\omega}_y\sin(\beta-\alpha) - sign(v_X)R_{air} \quad (9)$$

where r, β, and α are the IMU misalignments and μ is the drag coefficient.

C. *Using GA to fit $\bar{f}_{x_b}$ and f_{x_b} to identify the Parameters*

The main purpose of this section is to identify the parameters introduced in previous section: the IMU misalignments and the drag coefficient. The idea is that if the parameters are correct, the pseudo accelerations calculated by the proposed formula ($\bar{f}_{x_b}$) should be equal to the values measured by the accelerometer of x_b-axis (f_{x_b}). Accordingly, we use the difference between $\bar{f}_{x_b}$ and f_{x_b} as an error which should be optimized by GA while the parameters are tuned. This error is our Objective Function (OF) and is calculated using a root mean square error (RMSE) method as follows:

$$OF = \sqrt{\left(\frac{1}{n}\sum_{k=1}^{n}\left(f_{x_b(k)} - \bar{f}_{x_b(k)}\right)^2\right)} \tag{10}$$

Using equation above, GA attempts to fit $\bar{f}_{x_b}$ to the f_{x_b} by determining correct values for the IMU misalignments and the drag coefficient. As a result of this optimization, four parameters r, β, α, and μ are identified. Parameters r and β are used in rest of our study. We use parameters r and β to calculate the displacements of the vehicle's mass center with respect to the IMU's location. If some additional masses displace the center of mass, these parameters will be updated using the GA algorithm. This will make it possible to calculate the displacement.

D. *Estimating the location of the displaced Center of Mass*

Fig. 3 shows a situation in which an additional mass is being carried by the quadrotor. As shown in the figure, the center of mass is affected by the additional weight of the payload. r_0 in this figure shows the distance between the IMU and the center of mass. β_0 is the angle between r_0 and x_B-axis when there is no burden attached to the robot. In the case of a burden being carried by the quadrotor, the variables are r_{new} and β_{new}. l is the length of a vector from the previous center of mass to the new one and δ is its angle relative to the x_B-axis.

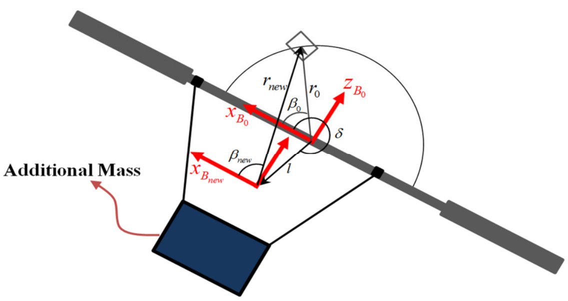

Fig. 3. The effect of an additional mass on the quadrotor's mass center

Having r_0, β_0, r_{new}, and β_{new} from the method introduced in the previous sections, the variables l and δ are calculated using equations below:

$$\begin{cases} l = \dfrac{r_0 \sin\left(\beta_{new} - \beta_0\right)}{\sin\left(\tan^{-1}\left(\dfrac{r_0 \sin\left(\beta_{new} - \beta_0\right)}{r_{new} - r_0 \cos\left(\beta_{new} - \beta_0\right)}\right)\right)} \\ \delta = \pi + \beta_{new} + \tan^{-1}\left(\dfrac{r_0 \sin\left(\beta_{new} - \beta_0\right)}{r_{new} - r_0 \cos\left(\beta_{new} - \beta_0\right)}\right) \end{cases} \tag{11}$$

IV. Test Strategy

In order to test the proposed algorithm it is necessary to displace the quadrotor's mass center by adding extra loads. In this test a lithium polymer battery, which adds 333 grams to the total mass of the quadrotor is located on the quadrotor. It has a considerable effect on the center of mass.

To estimate the approximate magnitude of mass center displacement, the quadrotor designed in Mechatronics Research Laboratory (MRL) is simulated in SolidWorks. Fig. 4 and Fig. 5 show the simulated quadrotor in two different modes. As Fig. 7 shows, in the first strategy the extra blue battery is located on the top of the quadrotor. In the second strategy, the battery is located beneath the quadrotor (Fig. 5).

According to the first strategy which is shown in Fig. 4, the center of mass is moved up and backward from its original location. In this mode the quadrotor's weight is 1.636 kg and its center of mass is at ($x_w = -0.489$ cm, $y_w = 0.165$ cm, $z_w = 5.053$ cm).

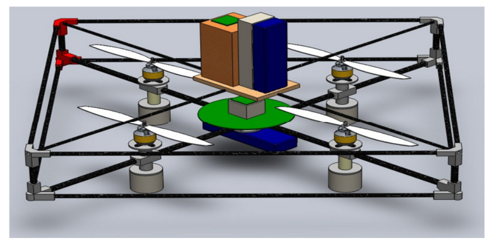

Fig. 4. The MRL's quadrotor modeled in SolidWorks

It can be seen in Fig. 5 that in the second strategy the additional battery is located beneath the primary battery. It should be noted that the batteries are located somehow in order to have a greater change in the location of the mass center. In this mode the quadrotor's weight is 1.633 kg and its center of mass is at ($x_w = 1.187$ cm, $y_w = 0.197$ cm, $z_w = 0.600$ cm).

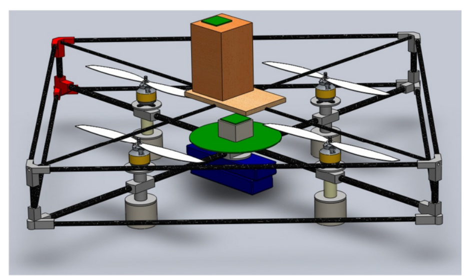

Fig. 5. The MRL's quadrotor modeled in SolidWorks

Calculating the mass center displacement from these configurations results ($\Delta x_w = 1.68\ cm$,$\Delta z_w = 4.45\ cm$). This means that the mass center is expected to be approximately displaced 1.68 cm along the x_b-axis and also 4.45 cm on the z_b-axis. These results will be compared to the results obtained from the experimental test.

V. Experimental Results

In this research a home-made quadrotor, which is shown in Fig. 6, is used as an experimental set up to test the theoretical ideas. First, the experimental setup including the system used to acquire data is introduced. Then, there will be the test results related to the two configurations shown in Fig. 4 and Fig. 5. Finally, mass center displacement is estimated.

A. Experimental Setup

The mechanical structure of the quadrotor which is used in this research is made of carbon fiber tubes and teflon joints. In order to stabilize the quadrotor, roll and pitch angles of the robot are controlled using MPC method. The yaw angle of the robot is also controlled using a PID controller. The main board of the robot is equipped with two ATMEGA128 microcontrollers. One of them is used only for implementation of the control algorithms and the other one is used for instrumentation system. An onboard XBee-PRO module is used for telecommunication of the robot and an RF remote controller is used for teleoperation.

The heart of the navigation system is a home-made IMU. The IMU has a three-axis accelerometer ADXL327, three-axis gyroscope ITG3200, and three-axis compass sensor HMC5843. The data acquired by this module are transferred to the main board via serial communication.

As Fig. 6 illustrates, two IMUs are used in the test. The first one is installed on the main board and is used to stabilize the robot. The second one which is located on the top of the quadrotor's mass center is dedicated for measuring the accelerations and turn rates used in our test.

B. Estimating the IMU Misalignments and the Drag Coefficient while the Center of Mass is displaced to an Upper Place

In this test, the additional battery is located on the top of the quadrotor's body. It is worth noting that the assumptions made in section III.B are considered in our tests. Fig. 6 shows the quadrotor configuration used for the first test.

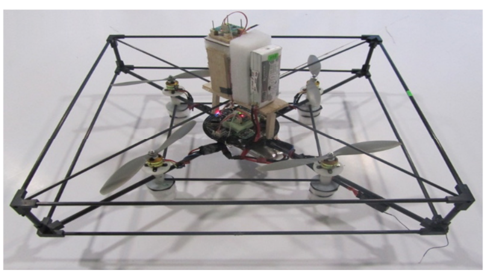

Fig. 6. The MRL's quadrotor (the first configuration)

The data which are collected for about 70 seconds during the robot's maneuver include:

- 1.5 seconds; motor off stationary
- 2 seconds; motor on stationary
- 9 seconds ; hovering without considerable movements
- 52 seconds; the main maneuver
- 4 seconds; landing
- 1 second; motor off stationary

In this maneuver the traveled path is along a 7 meter line in x_W direction which the quadrotor moves forward and backward for 8 laps. As one of our goals is to identify drag coefficient more precisely, we decided to move the robot as fast as possible in order to have more effective air resistance.

The acceleration and the angular velocity measured by the x_b-axis accelerometer and y_b-axis gyroscope are shown in Fig. 7 and Fig. 8, respectively.

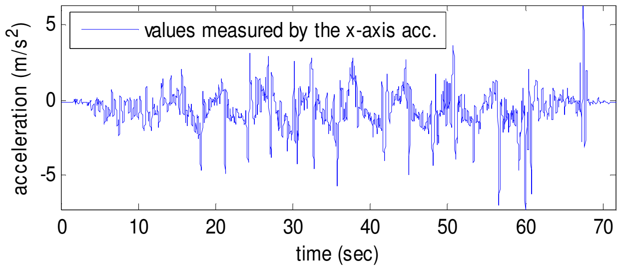

Fig. 7. Acceleration measured by the horizontal accelerometer

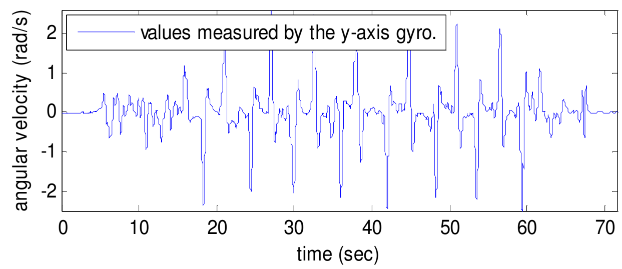

Fig. 8. Angular rate measured by the gyroscope

Using the collected data, the GA algorithm attempted to optimize the objective function. The GA population size was 250, and a scattered crossover function was used. The GA convergence diagram is shown in Fig. 9.

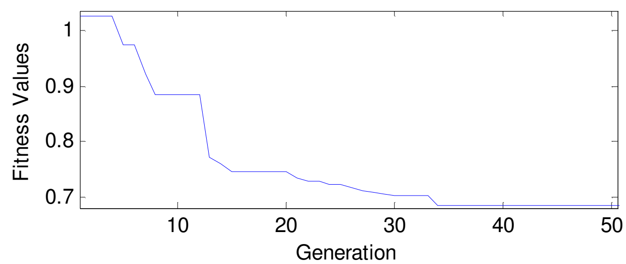

Fig. 9. The GA convergence curve while the objective function is being optimized

In this optimization, the obtained values of the parameters r, β, α, and μ are 0.19, 56.299, -2.812, and 0.0716, respectively. The optimized value of the OF is 0.677 (m/s^2). Since our test was offline and the GA was run on MATLAB, we were able to allow the GA to continue until the value of the OF became stable. However, the value 0.677 represents the mean error resulting from GA's optimization and depends on the accuracy of the sensory unit.

The identified parameters are used to calculate and compared $\bar{f}_{x_b}$ to the acceleration measured by the x_b-axis accelerometer (f_{x_b}). The result is shown in Fig. 10. As it can be seen from this figure, the acceleration calculated using the proposed GA-based formula is almost the same as the acceleration measured by the x_b-axis accelerometer and it can be inferred that the parameters r, β, α, and μ are estimated correctly.

C. Estimating the IMU Misalignments and the Drag Coefficient while the Center of Mass is displaced to a Lower Place

In the previous section, it was shown that the IMU misalignments and the drag coefficient can be identified using the proposed method. In this section, center of mass is displaced to a lower place and the test is repeated. Accordingly, it is expected to identify different parameters in this test.

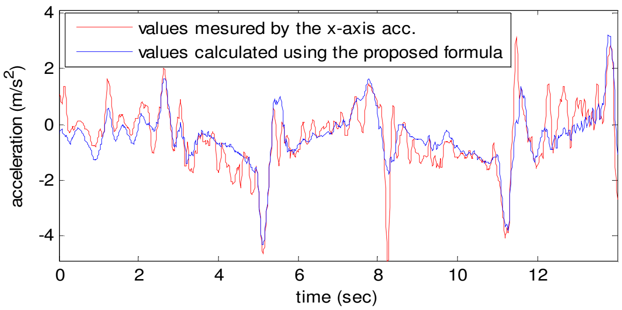

Fig. 10. A comparison of measured and calculated accelerations

Applying the same procedure explained in the previous section, while the additional battery is installed at the bottom of the quadrotor, the r, β, α, and μ are identified as 0.213, 66.066, -4.0132, and 0.107, respectively.

D. Calculating the mass center displacement

The IMU misalignments and the drag coefficient, (r, β, α, μ), for the first and the second quadrotor configurations were identified in the previous sections. In this section, r and β are used to calculate the mass center displacement. TABLE I shows these parameters for both tests. Using these values and the equation (11), the mass center displacement in Polar coordinates (l, δ) is obtained as (0.0413, 297.44). Transferring these values into Cartesian coordinate system results: ($\Delta x = 1.90\ cm$,$\Delta z = 3.66\ cm$). This shows that the center of mass is displaced with an amount of 1.90 (cm) in x_B direction and 3.66 (cm) in z_B direction after robot's reconfiguration.

TABLE I
IMU MISALIGNMENTS IDENTIFIED FROM THE TESTS

	SYMBOL	Estimated Value
Test1 [a]	r_0	0.19 (m)
	β_0	56.299 (deg)
Test2 [b]	r_{new}	0.213 (m)
	β_{new}	66.066 (deg)

VI. CONCLUSION

In this paper, it is shown that the quadrotor's horizontal accelerometers and gyroscopes can be used to calculate the location of the center of mass and the drag coefficient. Results show that the acceleration measured by a horizontal accelerometer is due to the IMU misalignments and the drag force. This is the idea used to identify the mentioned parameters using a GA-based algorithm. The identified parameters are used to calculate the mass center displacements in two different configurations in which the quadrotor's mass distribution is changed deliberately. Theoretical results are verified by the experimental results.

REFERENCES

[1] G. M. Hoffmann, H. Huang, S. L. Waslander, and C. J. Tomlin, "Quadrotor Helicopter Flight Dynamics and Control:Theory and Experiment," in AIAA Guidance, Navigation and Control Conference and Exhibit Hilton Head, South Carolina, 2007.

[2] Z. Fang and W. Gao, "Adaptive Integral Backstepping Control of a Micro-Quadrotor," in 2nd IEEE International Conference on Intelligent Control and Information Processing Shenyang, China, 2011, pp. 910-915.

[3] T. Bresciani, "Modelling, Identification and Control of a Quadrotor Helicopter," in Department of Automatic Control. vol. Master Thesis Lund: Lund University, 2008, p. 180.

[4] S. Bouabdallah, A. Noth, and R. Siegwart, "PID vs LQ Control Techniques Applied to an Indoor Micro Quadrotor," in IEEE International Conference on Intelligent Robots and Systems Sendai, Japan, 2004.

[5] A. Tayebi and S. McGilvray, "Attitude Stabilization of a Four-Rotor Aerial Robot," in 43rd IEEE Conference on Decision and Control Atlantis, Paradise Island, Bahamas, 2004, pp. 14-17.

[6] S. G. I.-V. Zquez and J. Moreno-Valenzuela, "A New Nonlinear PI/PID Controller for Quadrotor Posture Regulation," in IEEE Conference on Electronics, Robotics and Automotive Mechanics, 2010, pp. 642-647.

[7] J. Zhong, "PID Controller Tuning: A Short Tutorial," Mechanical Engineering, Purdue UniversitySpring, 2006.

[8] S. Bouabdallah, P. Murrieri, and R. Siegwart, "Design and Control of an Indoor Micro Quadrotor," in Robotics and Automation, 2004. Proceedings. ICRA '04. 2004 IEEE International Conference on. vol. 5, 2004 pp. 4393-4398.

[9] S. Seghour, M. Bouchoucha, and H. Osmani, "From integral backstepping to integral sliding mode attitude stabilization of a quadrotor system: Real time implementation on an embedded control system based on a dsPIC uC," in IEEE International Conference on Mechatronics, 2011, pp. 154-161.

[10] N. Abas, A. Legowo, and R. Akmeliawati, "Parameter Identification of an Autonomous Quadrotor," in 4th International Conference on Mechatronics, 2011, pp. 1-8.

[11] N. Michael, D. Mellinger, Q. Lindsey, and V. Kumar, "The GRASP Multiple Micro-UAV Test Bed: Experimental Evaluation of Multirobot Aerial Control Algorithms," in IEEE Robotics & Automation Magazine, September, 2010.

[12] P. Martin and E. Salaun, "The True Role of Accelerometer Feedback in Quadrotor Control," in 2010 IEEE International Conference on Robotics and Automation Anchorage Convention District Anchorage, Alaska, USA, 2010.

[13] H. Bouadi, S. S. Cunha, A. Drouin, and F. Mora-Camino, "Adaptive Sliding Mode Control for Quadrotor Attitude Stabilization and Altitude Tracking," in 12th IEEE International Symposium on Computational Intelligence and Informatics, 2011, pp. 449-455.

[14] M. Santos, V. L. pez, and F. Morata, "Intelligent Fuzzy Controller of a Quadrotor," in IEEE International Conference on Intelligent Systems and Knowledge Engineering, 2010, pp. 141-146.

[15] T. Raharijaona and F. Bateman, "Robust Control for an Off-Centered Quadrotor," in 19th Mediterranean Conference on Control & Automation, 2011, pp. 1253-1258.

[16] D. H. Titterton and J. L. Weston, Strapdown Inertial Navigation Technology: The Institution of Electrical Engineers (IEE), 2006.

[17] V. Khorani, A. Mohammad Shahri, S. M. R. Mirfakhar, and N. Ajilforoushan, "Effects of Quadrotor Motions on its Accelerometers: Theory and Simulation Results," in The Eighteenth Annual Conference on Mechatronics and Machine Vision in Practice (M2VIP'11) Brisbane, Australia, 2011.

[18] G. K. Batchelor, An introduction to fluid dynamics: Cambridge, England: Cambridge University Press, 1967.